

See discussions, stats, and author profiles for this publication at: <https://www.researchgate.net/publication/228068552>

# Macroporous Monolithic Methylsilsesquioxanes Prepared by a Two-Step Acid/Acid Processing Method

ARTICLE *in* CHEMISTRY OF MATERIALS · JULY 2006

Impact Factor: 8.35 · DOI: 10.1021/cm060509e

---

CITATIONS

26

---

READS

23

2 AUTHORS, INCLUDING:



Hanjiang Dong

Restek Corporation

15 PUBLICATIONS 263 CITATIONS

SEE PROFILE

# Macroporous Monolithic Methylsilsesquioxanes Prepared by a Two-Step Acid/Acid Processing Method

Hanjiang Dong and John D. Brennan\*

Department of Chemistry, McMaster University, Hamilton, Ontario L8S 4M1, Canada

Received March 2, 2006. Revised Manuscript Received May 28, 2006

The development of monolithic methylsilsesquioxane (MSQ) materials with bicontinuous meso-/macroporous morphologies has proven to be advantageous for the fabrication of chromatographic stationary phases. However, it is currently very difficult to obtain suitable columns over a range of capillary sizes, owing to alterations in morphology in narrow diameter capillaries and material shrinkage in large-bore capillaries. Herein, we describe a new acid/acid two-step sol–gel processing method (A2) for fabricating MSQ bicontinuous monolithic capillary columns with sizes ranging from 20 to 530  $\mu\text{m}$ . The effect of temperature on pore volume and pore size of the related bulk gel was characterized by mercury intrusion porosimetry. It was found that the pore morphologies are stable at 300  $^{\circ}\text{C}$  while pores contract significantly at 400  $^{\circ}\text{C}$ . The evolution of the MSQ chemical structure upon heat treatment was examined by infrared spectroscopy and thermogravimetric analysis. IR spectra demonstrate that both the unstable Si–C bonds (from  $\text{SiCH}_3$  groups) and the opening of rings at temperatures of 400  $^{\circ}\text{C}$  are responsible for the densification of gel skeletons and the collapse of macropores. These results indicate that column fabrication should be done without a calcining step to avoid irreversible loss of desirable morphologies and chemical properties.

## Introduction

Macroporous monolithic materials based on silica or organic polymers have attracted enormous interest as a platform for new chromatographic stationary phases.<sup>1</sup> The unique features of these materials include large throughpores ( $\sim$ micrometer scale) and tunable external porosities.<sup>2</sup> Organic polymer-based columns have been formed from polyacrylamide, polystyrene–divinylbenzene, polymethacrylate, and polyacrylate.<sup>1b,d,3</sup> The morphology of polymer-based monolithic stationary phases consists of poorly organized microglobules with large pores located among them and typically have a low surface area.<sup>2</sup> These materials are particularly well-suited for the separation of large molecules such as peptides, proteins, and nucleic acids<sup>4</sup> but are not ideal for small molecule separations. The drawbacks of these materials, which are typical of polymeric stationary phases, are low efficiency, poor mechanical rigidity, and swelling and shrinkage in organic solvents.<sup>5</sup>

Inorganic monolithic columns are usually prepared by poly(ethylene oxide) (PEO) induced phase separation of silica

sols followed by gelation, as described by Nakanishi et al.,<sup>6</sup> and have been adopted by Merck in Germany to make silica-based columns with the trade name Chromolith.<sup>7</sup> The sol–gel derived silica skeleton consists of a network of small, thin, and twisted threads, which also possess mesopores ( $\sim$ 10 nm) within the silica skeleton.<sup>8</sup> Additionally, the silica monoliths possess a very narrow distribution of both macropores and mesopores after post-structural modification steps such as etching and derivitization.<sup>8a</sup> These structural characteristics contribute to the ability to rapidly separate complex mixtures without losing resolution<sup>9</sup> and provide low hydraulic resistance to the movement of the mobile phase and an enhanced rate of mass transfer of the sample around the thin skeleton ( $\sim$ 1  $\mu\text{m}$ ).<sup>5</sup>

A key advantage of monolithic stationary phases is that they can be prepared directly in narrow-bore capillaries, which is difficult to do with particle-packed columns.<sup>10</sup> Technological advances in LC systems have resulted in the ability to accurately control low flow rates down to microliter

\* To whom correspondence should be addressed. Tel.: (905) 525-9140 (ext. 27033). Fax: (905) 527-9950. E-mail: brennanj@mcmaster.ca. Internet: <http://www.chemistry.mcmaster.ca/faculty/brennan>.

- (1) (a) Cabrera, K. *J. Sep. Sci.* **2004**, 27, 843. (b) Svec, F. *J. Sep. Sci.* **2004**, 27, 747. (c) Tanaka, N.; Kobayashi, H.; Nakanishi, K.; Minakuchi, H.; Ishizuka, N. *Anal. Chem.* **2001**, 73, 420A. (d) *Monolithic Materials: Preparation, Properties, and Applications*; Svec, F.; Tennikova, T. B.; Deyl, Z., Eds.; Elsevier: Amsterdam, 2003.
- (2) Svec, F.; Tanaka, N. *J. Sep. Sci.* **2004**, 27, 745.
- (3) Miller, S. *Anal. Chem.* **2004**, 76, 99A.
- (4) (a) Wang, Q.; Svec, F.; Frechet, J. M. J. *J. Chromatogr., A* **1994**, 669, 230. (b) Josic, D.; Buchacher, A. *J. Immunol. Methods* **2002**, 271, 47. (c) Xie, S.; Allington, R. W.; Svec, F.; Frechet, J. M. J. *J. Chromatogr., A* **1999**, 865, 169. (d) Oberacher, H.; Huber, C. G. *Trends Anal. Chem.* **2002**, 21, 166.
- (5) Miyabe, K.; Guiochon, G. *J. Sep. Sci.* **2004**, 27, 853.

- (6) (a) Minakuchi, H.; Nakanishi, K.; Soga, N.; Ishizuka, N.; Tanaka, N. *Anal. Chem.* **1996**, 68, 3498. (b) Minakuchi, H.; Nakanishi, K.; Soga, N.; Ishizuka, N.; Tanaka, N. *J. Chromatogr., A* **1997**, 762, 135. (c) Minakuchi, H.; Nakanishi, K.; Soga, N.; Ishizuka, N.; Tanaka, N. *J. Chromatogr., A* **1998**, 797, 121. (d) Ishizuka, N.; Minakuchi, H.; Nakanishi, K.; Soga, N.; Tanaka, N. *J. Chromatogr., A* **1998**, 797, 133.
- (7) (a) Bidlingmeyer, B.; Unger, K. K.; von Doehren, N. *J. Chromatogr., A* **1999**, 832, 11. (b) Cabrera, K.; Lubda, D.; Eggenweiler, H. M.; Minakuchi, H.; Nakanishi, K. *J. High Resolut. Chromatogr.* **2000**, 23, 93.
- (8) (a) Nakanishi, K. *J. Porous Mater.* **1997**, 4, 67. (b) Tallarek, U.; Leinweber, F. C.; Seidel-Morgenstern, A. *Chem. Eng. Technol.* **2002**, 23, 106.
- (9) (a) Tanaka, N.; Kobayashi, H.; Ishizuka, N.; Minakuchi, H.; Nakanishi, K.; Hosoya, K.; Ikegami, T. *J. Chromatogr., A* **2002**, 965, 35. (b) Motokawa, M.; Kobayashi, H.; Ishizuka, N.; Minakuchi, H.; Nakanishi, K.; Hosoya, K.; Ikegami, T.; Tanaka, N. *J. Chromatogr., A* **2002**, 961, 53.

or even nanoliter per minute levels, which allows monolithic capillary columns to be coupled to MS detectors without the need for flow splitting. The enhanced sensitivity and high throughput, resulting from narrow-bore columns with inner diameters as low as 20  $\mu\text{m}$ , has proven to be effective in drug screening and proteomics applications.<sup>11,12</sup>

While monolithic silica columns have proven to be useful for rapid and sensitive analysis of complex mixtures, several issues exist with the use of silica. First, syneresis during aging and shrinkage during drying make it impossible to prepare capillary-scale silica columns with sizes larger than 200  $\mu\text{m}$ . Second, according to our own experience, preparation of silica monolithic capillary columns with high reproducibility remains a significant challenge. This is in contrast to the situation with 4.6 mm i.d. columns, which show very good quality from batch to batch.<sup>13</sup> Third, the use of an organic polymer (PEO) to induce phase separation during the polymerization of tetramethoxysilane requires the removal of the polymer after gelation, which can alter the column properties. Finally, it is well-known that silica, even after modification with organosilanes, is not stable at either high (>8) or low (<2) pH.<sup>14</sup> These drawbacks call for the development of alternative materials, which ideally can overcome all of these issues.

Hybrid particle-packed columns containing Si–C bonds have demonstrated improved stability toward high pH, making them ideal for use at high pH to allow the separation of basic analytes.<sup>15</sup> We<sup>16</sup> and Nakanishi and co-workers<sup>17</sup> were the first to realize that the hydrophobic Si–CH<sub>3</sub> groups of methyltrimethoxysilane (MTMS) can initiate phase separation during its polymerization and make macroporous methylsilsesquioxane (MSQ) materials. This advantage makes the use of additives such as PEO unnecessary. The flexible gel network leads to much less shrinkage in MSQ monoliths compared to silica gels,<sup>18</sup> better stability to pH,<sup>16</sup> and high separation efficiency when operated in normal phase mode.<sup>18</sup> On the other hand, the lower degree of cross-linking relative to silica materials leads to structural deformation, which is induced by wetting of the sol–gel derived gelling phase by the confining capillary wall.<sup>19</sup> The extent of

structural deformation is enhanced as the ratio of the diameter of the capillary ( $D$ ) to the characteristic length of the bicontinuous structure of the bulk gel ( $\Lambda_m \sim 10 \mu\text{m}$ ) decreases. In extreme cases, the isotropic phase separation will break up when  $D/\Lambda_m < 1$ . As a result, it is very difficult to prepare small monolithic capillary columns with a diameter approaching 20  $\mu\text{m}$ . Improving the MSQ gel rigidity and/or reducing the feature size of MSQ monoliths are two approaches that should be able to overcome isotropic phase separation and should lead to columns with an inner diameter of 20  $\mu\text{m}$  or less.

Herein we describe a two-step process for the preparation of macroporous MSQ materials that utilizes an initial hydrolysis step done under weakly acidic conditions and a second step involving strong acid (A2 method). This method is based on our previously reported acid/base two-step process to prepare macroporous MSQ gels<sup>16,20</sup> but provides improvements in terms of controlling phase separation and gelation times and mechanical properties of the resulting MSQ materials, ultimately leading to reproducible bicontinuous structures even in very narrow capillaries. We show that such materials can be used to prepare MSQ capillary columns of various diameters ranging from 20 to 530  $\mu\text{m}$ , with good control over the final morphology. The physico-chemical properties of the MSQ materials were characterized by scanning electron microscopy (SEM), mercury porosimetry, IR, and thermogravimetric analysis (TGA), allowing us to assess the effect of column diameter and processing temperature on the characteristic length of the MSQ bicontinuous structure and the effect of temperature on the chemical structure of these materials.

While this work specifically addresses the application of MSQ materials as monolithic capillary columns, MSQ materials have been used in a wide variety of applications such as insulating coatings for optical and electrical devices,<sup>21</sup> additive powders to materials such as cosmetics, polypropylene films, and methacrylic resins,<sup>22</sup> and low dielectric films in the semiconductor industry.<sup>23</sup> Potential applications of these materials include superhydrophobic materials,<sup>24</sup> various separation media (solid-phase extraction,<sup>25</sup> lab-on-a-chip,<sup>26</sup> etc.), catalyst supports,<sup>27</sup> and matrixes for biomolecular entrapment.<sup>28</sup> Many of these applications require the

- (10) (a) Legido-Quigley, C.; Marlin, N. D.; Melin, V.; Manz, A.; Smith, Norman, N. W. *Electrophoresis* **2003**, *24*, 917. (b) Eeltink, S.; Decrop, W. M.; Rozing, G. P.; Schoenmakers, P. J.; Kok, W. T. *J. Sep. Sci.* **2004**, *27*, 1431.
- (11) (a) Barroso, B.; Lubda, D.; Bischoff, R. *J. Proteome Res.* **2002**, *1*, 459. (b) Premstaller, A.; Oberacher, H.; Walcher, W.; Timperio, A. M.; Zolla, L.; Chervet, J. P.; Cavusoglu, N.; van Dorsselaer, A.; Huber, C. G. *Anal. Chem.* **2001**, *73*, 2390.
- (12) (a) Luo, Q.; Shen, Y.; Hixson, K. K.; Zhao, R.; Yang, F.; Moore, R. J.; Mottaz, H. M.; Smith, R. D. *Anal. Chem.* **2005**, *77*, 5028. (b) Ivanov, A. R.; Zang, L.; Karger, B. L. *Anal. Chem.* **2003**, *75*, 5306.
- (13) Kele, M.; Guiochon, G. *J. Chromatogr., A* **2002**, *960*, 19.
- (14) Nawrocki, J.; Dunlap, C.; McCormick, A.; Carr, P. W. *J. Chromatogr., A* **2004**, *1028*, 1.
- (15) Wyndham, K. D.; O'Gara, J. E.; Walter, T. H.; Glose, K. H.; Lawrence, N. L.; Alden, B. A.; Izzo, G. A.; Hudalla, C. J.; Iraneta, P. C. *Anal. Chem.* **2003**, *75*, 6781.
- (16) (a) Dong, H.; Brook, M. A.; Brennan, J. D. *Chem. Mater.* **2005**, *17*, 2807. (b) Dong, H.; Reidy, F.; Brennan, J. D. *Chem. Mater.* **2005**, *17*, 6012.
- (17) (a) Nakanishi, K. *J. Sol-Gel Sci. Technol.* **2000**, *19*, 65. (b) Kanamori, K.; Ishizuka, N.; Nakanishi, K.; Hirao, K.; Jinnal, H. *J. Sol-Gel Sci. Technol.* **2003**, *26*, 157.
- (18) Kanamori, K.; Yonezawa, H.; Nakanishi, K.; Hirao, K.; Jinnal, H. *J. Sep. Sci.* **2004**, *27*, 874.
- (19) Kanamori, K.; Nakanishi, K.; Hirao, K.; Jinnal, H. *Colloids Surf., A* **2004**, *241*, 215.
- (20) Dong, H.; Brennan, J. D. *Chem. Mater.* **2006**, *18*, 541.
- (21) Baney, R. H.; Itoh, M.; Sakakibara, A.; Suzuki, T. *Chem. Rev.* **1995**, *95*, 1409.
- (22) Perry, R. J.; Adams, M. E. In *Silicones and Silicone-Modified Materials*; Clarkson, S. J., Fitzgerald, J. J., Owen, M. J., Smith, S. D., Eds.; American Chemical Society: Washington, DC, 2000; Vol. 728, p 533.
- (23) (a) Nguyen, C. V.; Kenneth, R. C.; Hawker, C. C.; Hedrick, J. L.; Jaffe, R. L.; Miller, R. D.; Remenar, J. F.; Rhee, H.-W.; Rice, P. M.; Toney, M. F.; Trollasa, M.; Yoon, D. Y. *Chem. Mater.* **1999**, *11*, 3080. (b) Yang, S.; Mirau, P. A.; Pai, C.-S.; Nalamasu, O.; Reichmanis, E.; Pai, J. C.; Obeng, Y. S.; Seputro, J.; Lin, E. K.; Lee, H.-J.; Sun, J.; Gidley, D. W. *Chem. Mater.* **2002**, *14*, 369. (c) Xu, J.; Moxom, J.; Yang, S.; Suzuki, R.; Ohdaira, T. *Appl. Surf. Sci.* **2002**, *194*, 189.
- (24) Shirlcliffe, N. J.; McHale, G.; Newton, M. I.; Perry, C. C. *Langmuir* **2003**, *19*, 5626.
- (25) (a) Shintani, Y.; Zhuo, X.; Furuno, M.; Minakuchi, H.; Nakanishi, K. *J. Chromatogr., A* **2003**, *985*, 351. (b) Miyazaki, S.; Morisato, K.; Ishizuka, N.; Minakuchi, H.; Shintani, Y.; Furuno, M.; Nakanishi, K. *J. Chromatogr., A* **2004**, *1043*, 19.

control of gel morphology, as discussed in this paper. The other issue we address in this work is the rigidity of porous sol–gel derived materials. High mechanical strength is critical to sol–gel material processing (e.g., rapid drying, reducing shrinkage, and avoidance of cracking) and applications such as aerogels<sup>29</sup> and low- $k$  dielectrics.<sup>30</sup> Thus, methods to increase gel rigidity are required.

## Experimental Section

**Chemicals.** All chemicals, including MTMS, nitric acid (HNO<sub>3</sub>), hydrochloric acid (HCl), and methanol (MeOH) were of analytical grade or above and were purchased from Aldrich (Ontario, Canada). All reagents were used as received. All water was obtained from a Milli-Q Synthesis A10 water purification system. Fused-silica capillary tubing was purchased from Polymicro (AZ).

**Procedures.** *Sample Preparation.* MSQ bulk gels or monolithic columns were prepared using 1 mL of MTMS + 0.283 mL of MeOH + 0.05 mL of 0.01 M HCl + 0.20 mL of 1.0 M HNO<sub>3</sub>. First, MTMS, MeOH, and 0.01 M HCl were mixed for 1 h ( $t_{\text{acid1}}$ ) at room temperature (ca. 20 °C) to promote hydrolysis and early stage condensation reactions, after which 1.0 M HNO<sub>3</sub> was added to the solution to promote hydrolysis and accelerate condensation reactions. About 10 min after adding 1.0 M HNO<sub>3</sub>, the MSQ sol was pushed into the capillary by hand using a 3 mL syringe. The gelation time and phase separation time were taken from the point where 1.0 M HNO<sub>3</sub> was added. After gelation, the bulk samples and columns were aged at room temperature for 1 day and then 70 °C for 1 day and finally were dried at 120 °C for 1 day.

*Characterization of Monolithic Materials.* Images of gels were obtained using a Philips 515 scanning electron microscope at an operating voltage of 20 kV. The surfaces were previously sputter-coated with gold to avoid charging effects during observation. Porosity measurements were performed by mercury porosimetry using a Quantachrome PoreMaster GT over a pressure range of 60–60 000 psi. All samples were degassed at 150 °C or above for at least 10 h before measurement. Samples were prepared for Fourier transform infrared (FTIR) spectroscopy by crushing the dried gels to a fine powder in a mortar, mixing thoroughly with powdered KBr at a ratio of 1 part sample to 150 parts KBr by weight, and pressing into a 0.5 mm thick disk. Transmission spectra were measured with a Bio-Rad FTS-40 spectrometer. Each spectrum represents the average of 32 scans with a 2 cm<sup>−1</sup> spectral resolution from 4000 to 400 cm<sup>−1</sup>. TGA was performed on a NETZSCH STA 409 instrument in the range of 70–600 °C, with a heating rate of 2 °C/min, under 50 mL·min<sup>−1</sup> air flux.

## Results and Discussion

In previous studies we described a two-step acid/base (B2) processing method for forming macroporous MSQ materials.

While this method provided good control over the morphology of the resulting material, the difference in gelation and phase separation times, defined as the coarsening time, was only 7–10 min, which led to issues with reproducibility in terms of morphology of the material. Furthermore, the B2 method uses volatile NH<sub>4</sub>OH as the catalyst, the concentration of which changes with time and leads to a further source of irreproducibility, which makes it difficult to consistently obtain bicontinuous morphologies in narrow-bore capillaries.

To overcome these drawbacks, we investigated the use of a two-step acid/acid processing method with lower water and cosolvent concentrations using molar ratios of MTMS/MeOH/0.01 M HCl/1.0 M HNO<sub>3</sub> = 1:1:0.4:1.6. On the basis of previous experiments,<sup>20</sup> a duration of 1 h was selected for the first weakly acidic hydrolysis step, which leads to the formation of a significant amount of MSQ oligomers. Nakanishi and co-workers have previously shown that MSQ monolithic columns prepared by the hydrolysis and condensation of MTMS under strongly acidic one-step processing conditions exhibit no shrinkage up to 530 μm,<sup>18</sup> which is not possible for silica gels. Nevertheless, structural deformation occurs as the column size diminishes, and it is very hard to prepare well-preserved bicontinuous structures in a 20 μm capillary using one-step processing conditions.<sup>19</sup> As discussed in the introduction, there are two possible solutions to prepare columns with an inner diameter of 20 μm. One is to increase the rigidity of the gel network, and the other is to decrease the characteristic size of the bicontinuous structure. Our previous report established that the size of oligomers and their distribution formed in the acidic step can effectively control the final morphology of MSQ materials prepared by the B2 method.<sup>20</sup> We also pointed out that MSQ developed a more rigid gel under B2 conditions than under one-step basic conditions.<sup>16a</sup> With this in mind, we developed a two-step processing method (A2), where the oligomers formed in the first weakly acidic step are used to control MSQ gel morphology and rigidity to make ultrasmall size columns, while retaining the advantage of strongly acidic conditions in the second step to provide superior shrinkage resistance and allow the fabrication of wide-bore columns.

Both the gelation time ( $t_g$ ) and phase separation time ( $t_{ps}$ ) are key parameters that control the final morphology of sol–gel derived materials, and these parameters have been extensively studied by Nakanishi for sol–gel derived silica materials.<sup>8</sup> The terms “gelation time” and “phase separation time” refer to the times for the reaction mixture to lose flow and to undergo microscale phase separation, as evidenced by the appearance of opaqueness, respectively. In our system, both values are measured from the time when 1.0 M HNO<sub>3</sub> is added. In this particular case,  $t_{ps}$  and  $t_g$  are about 55 min and 5 h and 10 min, respectively, resulting in a difference (coarsening time) of 4 h and 15 min. In the one-step processing method, these values are 2 h and 3 h and 4 min, respectively.<sup>18</sup> Our  $t_g - t_{ps}$  is significantly higher than that obtained using the B2 method (<10 min) and when using only one-step processing with 1.0 M HNO<sub>3</sub> as the catalyst (1 h and 4 min). It is interesting that such a long coarsening time in the A2 method leads to a similar MSQ morphology (pore and skeleton sizes, see Figure 1) as was obtained by

- (26) Breadmore, M. C.; Shrinivasan, S.; Wolfe, K. A.; Power, M. E.; Ferrance, J. P.; Hostica, B.; Norris, P. M.; Landers, J. P. *Electrophoresis* **2002**, *23*, 3487.
- (27) Reetz, M. T.; Zonta, A.; Simpelkamp, J. *Angew. Chem., Int. Ed. Engl.* **1995**, *34*, 301.
- (28) (a) Lee, M.-Y.; Park, C. B.; Dordick, J. S.; Clark, D. S. *Proc. Natl. Acad. Sci. U.S.A.* **2005**, *102*, 983. (b) Tripathi, V. S.; Kandimalla, V. B.; Ju, H. *Sens. Actuators, B* **2006**, *114*, 1071.
- (29) (a) Einarssrud, M.-A. *J. Non-Cryst. Solids* **1998**, *225*, 1. (b) Ma, H. S.; Prévost, J. H.; Jullien, R.; Scherer, G. W. *J. Non-Cryst. Solids* **2001**, *285*, 216. (c) Woignier, T.; Reynes, J.; Hafidi Alaoui, A.; Beurroies, I.; Phalippou, J. *J. Non-Cryst. Solids* **1998**, *241*, 45. (d) Gross, J.; Scherer, G. W. *J. Sol.-Gel. Sci. Technol.* **1998**, *13*, 957.
- (30) Mosig, K.; Jacobs, T.; Brennan, K.; Rasco, M.; Wolf, J.; Augur, R. *Microelectron. Eng.* **2002**, *64*, 11.



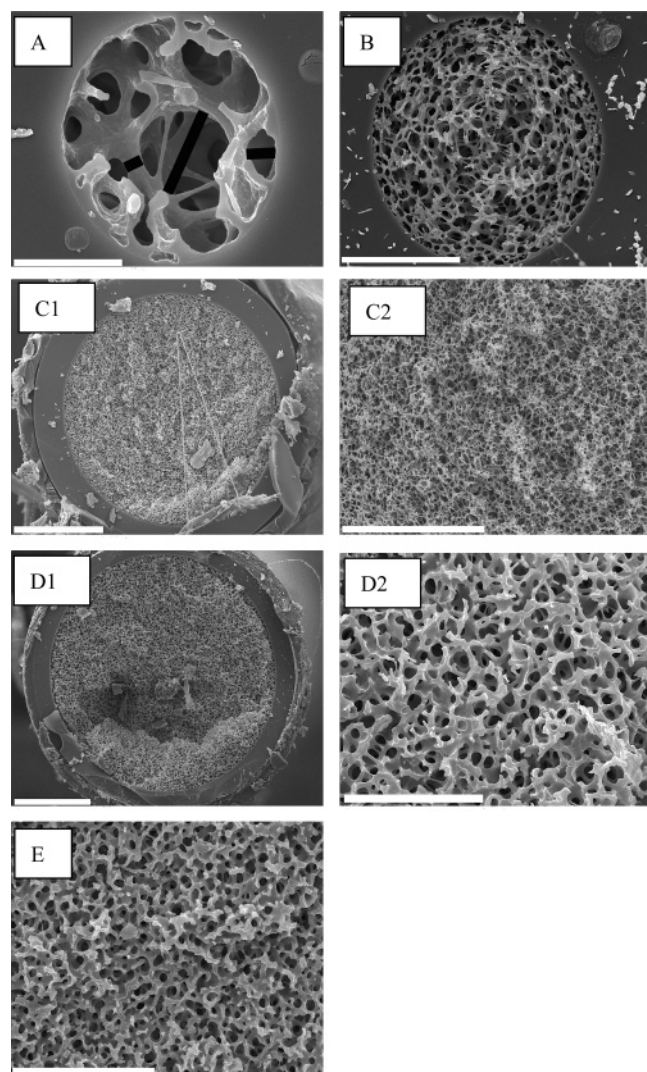


**Figure 1.** SEM images of MSQ monoliths. Panels A–D correspond to capillary i.d. values of 20, 100, 250, and 530  $\mu\text{m}$ , respectively. Panel E is a bulk gel. Bars (white): (A) 10  $\mu\text{m}$ , (B) 50  $\mu\text{m}$ , (C1) 100  $\mu\text{m}$ , (C2) 50  $\mu\text{m}$ , (D1) 200  $\mu\text{m}$ , (D2) 50  $\mu\text{m}$ , and (E) 50  $\mu\text{m}$ . In panel A, the three black bars are skeleton width (SW, shortest), pore width (PW, intermediate), and pore length (PL, longest).

the B2 method with a much shorter coarsening time (see Figure 2, panels C, E, and F, in ref 20). The fact that the gelation occurs several hours after phase separation when using the A2 method provides a key advantage over the B2 method: increased reproducibility. Small variations in either temperature or humidity can often lead to a significant difference in  $t_g/(t_g - t_{ps})$  and, therefore, drastic structural changes of MSQ monoliths obtained by the B2 method; this was not the case for the A2 method.

SEM images of MSQ bulk monoliths and columns with different inner diameters were obtained after MSQ materials were dried at 120  $^{\circ}\text{C}$  for 1 day and are shown in Figure 1. It is clear that MSQ materials derived by the A2 method exhibit no radial shrinkage and are crack-free in all columns, highlighting MSQ as a potential material for the development of monolithic columns. All samples display a network with strands of solid phase (skeleton) joined at nodes. A node is usually comprised of 3–6 skeletons. To evaluate the influence of the capillary sizes on the structural features of MSQ materials, we calculated the pore width (PW), pore length

**Table 1.** Effect of Column Sizes and Temperatures on the Characteristic Structures of MSQ Gels<sup>a</sup>

	sample							
	C20 <sup>b</sup>	C100	C250	C530	B120 <sup>c</sup>	B300	B400	B450
SW	1.41	1.29	0.58	1.98	1.53	1.59	1.22	1.03
PL	3.91	2.98	1.17	3.69	2.18	2.15	2.01	1.45
PW	2.67	1.96	0.84	2.89	1.65	1.59	1.55	1.07

<sup>a</sup> SW, skeleton width; PL, pore length; PW, pore width ( $\mu\text{m}$ ). <sup>b</sup> In the C series, C means column, which is followed by the column diameter in micrometers. Thus, C20 represents a 20  $\mu\text{m}$  capillary column. <sup>c</sup> In the B series, B means bulk, and the number which follows refers to the processing temperature. Thus, B300 represents a bulk monolith after heat treatment at 300  $^{\circ}\text{C}$ .

(PL), and skeleton width (SW). An example of the PW, PL, and SW is given in Figure 1, panel A. The average SW, PW, and PL, which are listed in Table 1, are measured directly from the SEM images using 25 data points (20  $\mu\text{m}$  column) or 50 data points (all other samples). From Table 1, it is clear that increases in column size from 20 to 250  $\mu\text{m}$  diameter result in decreases in the feature sizes. However, increasing to 530  $\mu\text{m}$  capillaries results in a large increase in SW, PL, and PW, which are even bigger than the values obtained for the bulk gel. Nakanishi and co-workers have shown that alteration of the capillary or channel width can produce significant alterations in the morphology of monolithic silica and MSQ materials owing to interactions between the material and the support wall, which are reduced in wider diameter supports.<sup>17,18</sup> However, these interactions are important only when the feature sizes of the monoliths are comparable to the length scale of the confined surroundings, which is usually much less than 50  $\mu\text{m}$ . Therefore, the changes of morphology observed for MSQ materials when capillary inner diameters reach 250  $\mu\text{m}$  are unexpected, and the reasons for these changes remain unclear.

A key point to note from the SEM data is that the pores are anisotropic, ranging from 1.27 (PL/PW) in 530  $\mu\text{m}$  columns to 1.52 in 100  $\mu\text{m}$  columns. This may result from local variations in the silica concentration when porous structures are frozen at the gelation point. While SEM provides only a two-dimensional representation of the pore structure, it is notable that three-dimensional images of sol-gel derived macroporous materials, which have been reconstructed from two-dimensional sliced images obtained from laser scanning confocal microscopy, correlate well with SEM images in terms of pore and skeleton morphology.<sup>18,19</sup> Thus, even though SEM refers to planar dimensions, these are representative of the three-dimensional structure of the monolithic material.

Mercury intrusion porosimetry data of bulk gels, which provides information on the sizes of macropores and mesopores (bigger than 3.5 nm) in the MSQ materials, are shown as a function of processing temperature in Figure 2. Differential pore size distributions show that there are no mesopores larger than 3.5 nm in A2 derived MSQ macroporous materials. However, this does not necessarily indicate an absence of mesopores in the original material because the high pressures used to measure the smallest mesopores may lead to compression of the material and mesopore collapse. Attempts to measure the mesopore properties using nitrogen sorption led to curves that did not close at low

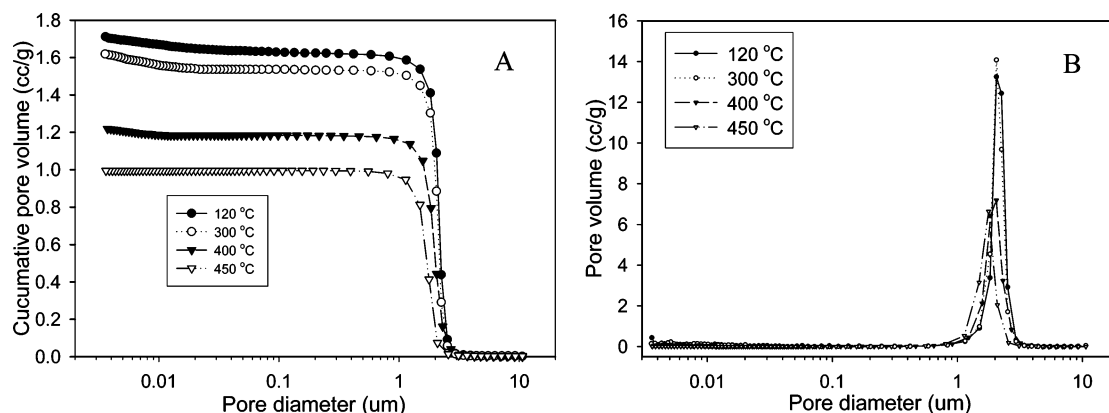


**Figure 2.** Effect of temperature on cumulative (A) and differential (B) pore size distribution of MSQ bulk gels. The measurements were carried out by mercury porosimetry.

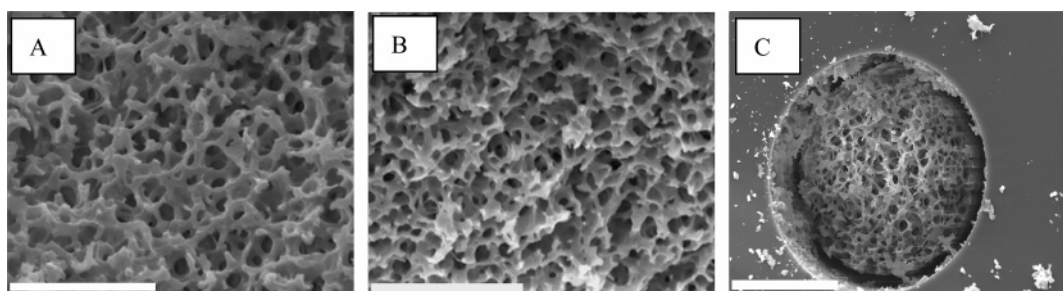
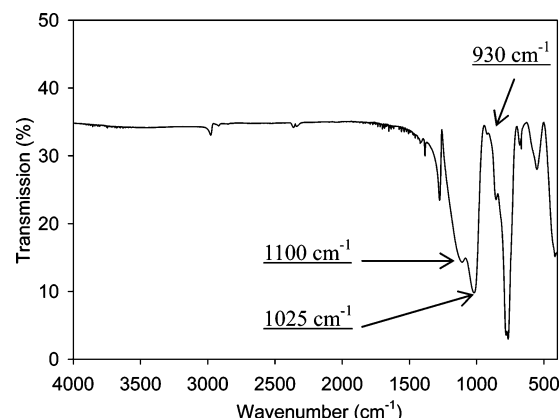


**Figure 3.** SEM images of MSQ bulk gels or monolithic columns at different temperatures. (A) Bulk gel at 300 °C, bar = 20  $\mu\text{m}$ ; (B) bulk gel at 450 °C, bar = 20  $\mu\text{m}$ ; and (C) 100  $\mu\text{m}$  column at 450 °C, bar = 50  $\mu\text{m}$ .

pressure (data not shown), making it impossible to accurately measure the mesoporosity. Sample swelling and the presence of micropores may account for this odd low-pressure hysteresis, as previously proposed.<sup>20</sup> However, further investigation is required to clarify this phenomenon.

Considering the macropore properties, our data show that the MSQ bulk samples processed at 120 °C exhibit a pore size distribution from 0.83 to 3.40  $\mu\text{m}$  which is centered at 2.10  $\mu\text{m}$ . When the temperature is raised from 120 to 300 °C, the total pore volume decreases from 1.71 to 1.62  $\text{cm}^3/\text{g}$ , while the pore size becomes slightly sharper and the pore size distribution becomes slightly narrower. Further increases in temperature to 400 °C result in a significant decrease in pore volume, and raising the temperature to 450 °C causes the total pore volume to decrease to only 60% of the value at 120 °C. Processing at 450 °C also causes a decrease in the mean pore size from 2.10 to 1.70  $\mu\text{m}$  and results in noticeable shrinkage of the bulk monolith (usually linear shrinkage around 15%), which begins at temperatures higher than 400 °C. Figure 3, panel C, shows that such temperatures cause MSQ gels inside capillaries to pull away from the capillary wall as a result of shrinkage. This is due to densification of the gel skeleton and the collapse of pores.

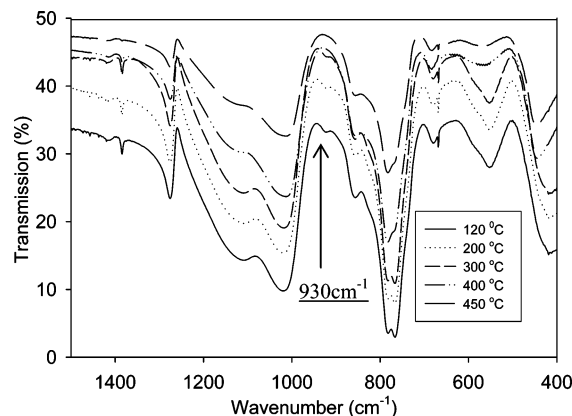
Changes of the feature sizes, based on SEM images, are summarized in Table 1 from B120 to B450 and are in general agreement with the mercury porosimetry results. Up to 300 °C, SW, PL, and PW show no change relative to 120 °C, while these values decrease significantly at a processing temperature of 450 °C. While all pores shrink (see also Figure 3, panels A and B), it seems that larger pores contract first. This phenomenon has previously been observed during sintering of silica aerogels,<sup>31</sup> although the driving force for



**Figure 4.** FTIR spectrum of a MSQ bulk gel dried at 120 °C. The Si—O—Si asymmetric stretching modes of the cyclic and polycyclic species at 1100  $\text{cm}^{-1}$  and of the linear and branched species at 1025  $\text{cm}^{-1}$  and the Si—OH stretching mode at 930  $\text{cm}^{-1}$  are highlighted (see Figure 5 for a better view of the latter peak and the text for a discussion of these bands).

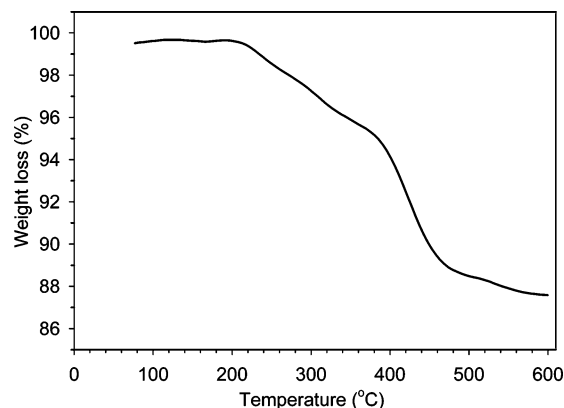
this phenomenon in MSQ materials may be different. In addition, the MSQ material loses its elastic nature and becomes brittle, which can be easily verified by breaking the sample by hand. Chemical reactions responsible for these changes are discussed below on the basis of FTIR and TGA data.

Figure 4 shows a FTIR spectrum of an MSQ bulk gel dried at 120 °C, while Figure 5 shows the FTIR spectra of the same bulk gel as a function of processing temperature. As can be seen from Figure 4, the dominant Si—O—Si asymmetric stretching mode is split into doublets, which are located at around 1110 and 1025  $\text{cm}^{-1}$ . The frequency at



**Figure 5.** FTIR spectra of a MSQ bulk gel at different temperatures in the wavenumber range of 1500–400  $\text{cm}^{-1}$ .

1110  $\text{cm}^{-1}$  is characteristic of the absorption of polycyclic oligomers  $(\text{CH}_3\text{SiO}_{3/2})_n$ ,<sup>32</sup> where  $n = 8, 10$ , and 12, indicative of the presence of cyclic and polycyclic units in the MSQ gels. The band at 555  $\text{cm}^{-1}$  is due exclusively to a Si–O–Si symmetric stretching vibration for a 4-silicon ring.<sup>33</sup> The asymmetric stretching band at 1025  $\text{cm}^{-1}$  arises from the resonance of linear and branched silicon species while its corresponding symmetric stretching mode is located at 680  $\text{cm}^{-1}$ . The peak at 440  $\text{cm}^{-1}$  is attributed to O–Si–O bending. The intensity of the 1025  $\text{cm}^{-1}$  band (due to linear and branched species) is stronger than that of the 1110  $\text{cm}^{-1}$  band (due to cyclic and polycyclic species) in the A2-derived MSQ gels. This structural feature makes MSQ gels prepared using the A2 method similar to those obtained using the B2 method. In contrast, the intensity of the band at 1110  $\text{cm}^{-1}$  is higher than that at 1025  $\text{cm}^{-1}$  in an MSQ gel obtained under weakly acidic conditions.<sup>16a,34</sup> Although it is well-established that intramolecular condensation (cyclization) can effectively compete with intermolecular reactions in the presence of an acid and that cyclization is suppressed under basic conditions during polymerization of silicon alkoxides, previous investigations (mainly by NMR and MS) were mostly conducted under weakly acidic and basic conditions (pH from 2 to 10).<sup>35</sup> Our result indicates that the reaction pathways of MTMS (and probably other silicon alkoxides) under strongly acidic conditions may be different because of the pH effect. Alternatively, this may result from the much higher concentration of the precursor because intermolecular condensation requires diffusion while cyclization does not. Therefore, high concentrations of MTMS may promote the reaction pathways for chain extension and the formation of branched species due to the diffusion effect.



**Figure 6.** TGA curve of a MSQ sample previously dried at 120  $^{\circ}\text{C}$  under an air atmosphere.

There are several low-intensity bands resulting from the residual groups of Si–OH and Si–OCH<sub>3</sub> groups in A2 derived MSQ materials. The Si–OH groups lead to a broad O–H stretching band ranging from 3000 to 3700  $\text{cm}^{-1}$  and a small shoulder due to Si–OH stretching at 930  $\text{cm}^{-1}$ . Both the Si–O and the C–H stretching modes in Si–OCH<sub>3</sub> groups are characteristic and located at 1085 and 2850  $\text{cm}^{-1}$ , respectively.<sup>36</sup> However, these peaks are very weak, and the former frequency is overlapped with the strong Si–O–Si asymmetric stretching peaks, which can only be resolved by a high-resolution instrument.

The remaining bands in Figure 4 are involved in the Si–CH<sub>3</sub> groups. Asymmetric and symmetric stretching vibrations of C–H bonds are at 2975 and 2919  $\text{cm}^{-1}$  (very weak), respectively. The corresponding asymmetric and symmetric deformation modes are located at 1385 and 1275  $\text{cm}^{-1}$  (very sharp), respectively. The two strong components at 768 and 780  $\text{cm}^{-1}$  arise from the combination of the methyl rocking modes and asymmetric stretching of Si–C in a C–Si–O unit, while the shoulder at 856  $\text{cm}^{-1}$  is due to CH<sub>3</sub> rocking.<sup>34a</sup>

To better understand the effect of temperature on the structural evaluation of MSQ materials as a function of time, a TGA experiment was performed for a 120  $^{\circ}\text{C}$  dried gel, as shown in Figure 6, and the weight losses were correlated to FTIR data, shown in Figure 5. The TGA curve shows that weight loss before 200  $^{\circ}\text{C}$  is less than 1%, indicating that the sample was essentially dry after heating at 120  $^{\circ}\text{C}$  for 1 day and that there are no chemical reactions occurring up to 200  $^{\circ}\text{C}$  in the MSQ samples. The former is in sharp contrast with the results for silica gels, in which physically adsorbed water cannot be completely removed even at much higher temperatures. The difference can be attributed to the hydrophobic Si–CH<sub>3</sub> groups on the MSQ surface, which prevent strong interactions with water through hydrogen bonding. The weight loss from 200 to 300  $^{\circ}\text{C}$  is about 2%. Figure 5 illustrates that there is no obvious change in the intensity at 930  $\text{cm}^{-1}$  because of the stretching mode of Si–O in the residual Si–OH groups, indicating their stability up to this temperature. The same is true for the cyclic species because the vibrations at 1110 and 550  $\text{cm}^{-1}$  have almost identical intensities. In contrast, redistribution reactions involving the

- (32) (a) Voronkov, M. G.; Lavrent'yev, V. I. *Top. Curr. Chem.* **1982**, *102*, 199. (b) Vogt, L. H., Jr.; Brown, J. F., Jr. *Inorg. Chem.* **1963**, *2*, 189.  
 (33) Smith, A. L. *Spectrochim. Acta* **1963**, *19*, 849.  
 (34) (a) Capozzi, C. A.; Pye, L. D.; Condrate, R. A., Sr. *Mater. Lett.* **1992**, *15*, 130. (b) Huang, Q. R.; Volksen, W.; Huang, E.; Tony, M.; Frank, C. W.; Miller, R. D. *Chem. Mater.* **2005**, *14*, 3676. (c) Liu, W. C.; Yang, C. C.; Chen, W. C.; Dai, B. T.; Tasi, M. S. *J. Non-Cryst. Solids* **2002**, *311*, 233.  
 (35) (a) Devereux, F.; Boilot, J. P.; Chaput, F. *Phys. Rev. A* **1990**, *41*, 6901. (b) Rankin, S. E.; Macosko, C. W.; McCormick, A. V. *AIChE J.* **1998**, *44*, 1141. (c) Dong, H.; Lee, M.-H.; Thomas, R. D.; Zhang, Z.; Reidy, R. F.; Mueller, D. W. *J. Sol.-Gel Sci. Technol.* **2003**, *28*, 5. (d) Kim, H.-J.; Lee, J.-K.; Park, S.-J.; Ro, H. W.; Yoo, D. Y.; Yoon, D. Y. *Anal. Chem.* **2000**, *72*, 5673. (e) Wallace, W. E.; Guttman, C. M.; Antonucci, J. M. *J. Am. Soc. Mass Spectrom.* **1999**, *10*, 224.

- (36) Lipp, E. D.; Smith, A. L. In *The Analytical Chemistry of Silicones*; Smith, A. L., Ed.; John Wiley & Sons: New York, 1991; p 305.



transformation of cyclic and polycyclic species into linear and branched species in MSQ materials developed under weakly acidic conditions occur well below 300 °C.<sup>34b</sup> MS spectra validate that the weight loss in this temperature range is mainly involved with the residual Si—OCH<sub>3</sub> groups through the formation of either methanol or methane.<sup>37</sup>

The weight loss from 300 to 400 °C is about 3%. There are several significant changes in the IR spectra after 300 °C. The band at 930 cm<sup>-1</sup> disappears. The 1025 cm<sup>-1</sup> mode grows and becomes broader at the expense of the 1110 cm<sup>-1</sup> band. The vibration at 550 cm<sup>-1</sup> diminishes in concert with the 1110 cm<sup>-1</sup> band. The frequency at 430 cm<sup>-1</sup> is shifted to 460 cm<sup>-1</sup>. The intensity of the double peaks at 782 and 768 cm<sup>-1</sup> bands reverses. Last, the band intensity at 1270 and 1430 cm<sup>-1</sup> is reduced. This signifies that several reactions occur simultaneously in this temperature range, which are interpreted as follows. First of all, condensation reactions involving Si—OH groups continue as the temperature increases. At 400 °C, it is obvious that the MSQ gel is fully condensed. Ring opening or redistribution reactions account for the changes in intensity for the bands at 1110, 1025, and 550 cm<sup>-1</sup>. It is a little surprising that Si—CH<sub>3</sub> groups are unstable at 400 °C for the MSQ macroporous materials, given that previous investigations revealed Si—CH<sub>3</sub> groups in thin films to be stable up to at least 450 °C.<sup>38</sup> The loss of CH<sub>3</sub> groups is directly responsible for the reduced intensity of peaks at 1270 and 1430 cm<sup>-1</sup>. It is also the reason the intensity of the band at 780 cm<sup>-1</sup> becomes much stronger than that at 768 cm<sup>-1</sup> and the O—Si—O bending mode at 430 cm<sup>-1</sup> shifts to a higher frequency. These changes can be explained by the formation of silica domains in the MSQ matrix. Ring opening and the initial loss of Si—CH<sub>3</sub> groups lead to densification of the gel skeleton network and collapse of the pore network. Therefore, IR and TGA data provide diagnostic support for the mercury porosimetry results. Weight loss from 400 to 600 °C is roughly 6.5%, giving a total of 12.5%. As can be seen from the IR spectra, the major change above 400 °C is the continuing loss of CH<sub>3</sub> groups.

Taken together, the results of the porosimetry, SEM, IR, and TGA data show that MSQ materials eventually transform to pure silica as the temperature is increased, with significant chemical transformations and alterations in morphology beginning at temperatures above 300 °C. Two of the key advantages of MSQ materials are their low degree of shrinkage and resistance to pH, both of which are the result of Si—CH<sub>3</sub> groups in the material. Hence, it is clear that processing of MSQ columns must be done at temperatures

below 300 °C to retain the methyl groups. On the other hand, processing at a temperature of 300 °C does not lead to significant densification of the material, which should increase the overall mechanical robustness of the material. Even so, this processing temperature retains a fraction of the Si—OH groups that could be further derivatized to form reversed phase columns.

While the current study provides important data for fabrication of MSQ stationary phases, further work is needed to examine the potential of these materials for both normal and reversed phase chromatography. Issues related to control of mesoporosity, ability to effectively derivatize residual Si—OH groups, and actual performance in the separation of compounds must be evaluated and will form the basis of future studies.

## Conclusions

This paper introduces an acid/acid two-step processing (A2) method to prepare macroporous MSQ materials. The new method uses the preformed oligomers of the first step to control the MSQ morphology and permits the fabrication of monolithic capillary columns with a well-defined network structure without shrinkage and cracking up to a size of 530 μm. Significantly, we are able to show that MSQ hybrid materials display little structural deformation in a small 20 μm column. The average skeleton width, pore width, and pore length range from 0.58 to 1.98, 0.84 to 2.67, and 1.17 to 3.91 μm, respectively. However, there is no single trend that can describe the effect of column size on the MSQ feature sizes. We are currently evaluating the performance of these columns for the separation of a range of compounds and are also developing even smaller i.d. columns to probe the minimum column diameter that will support a bicontinuous morphology.

The extent of cyclization in the macroporous MSQ materials prepared by the A2 method is similar to that obtained by acid/base two-step processing. These monoliths are fairly stable at 300 °C. Ring opening and thermal decomposition of SiCH<sub>3</sub> groups beginning above 300 °C are responsible for the drastic change of the morphology (decrease of pore and skeleton sizes). This indicates that column processing must be done at temperatures of 300 °C or below.

**Acknowledgment.** The authors thank the Natural Sciences and Engineering Research Council of Canada, MDS-Sciex, the Canadian Foundation for Innovation, and the Ontario Innovation Trust for financial support of this work. J.D.B. holds the Canada Research Chair in Bioanalytical Chemistry.

(37) Abe, Y.; Kagayama, K.; Takamura, N.; Gunji, T.; Yoshihara, T.; Takahashi, N. *J. Non-Cryst. Solids* **2000**, *261*, 39.

(38) Huang, Q. R.; Frank, C. W.; Mecerreyes, D.; Volksen, W.; Miller, R. D. *Chem. Mater.* **2005**, *17*, 1521 and references therein.